Malaysian Journal of Chemistry, 2026, Vol. 28(3), 112-125
(Special Issue: *International Conference on Chemistry and Sustainability, IC-CS 2025*)

Synthesis and Performance of Green Synthesized CuO Nanoparticles for Degradation of Noxious Bromocresol Green

Shilpi, Avantika, Anamika and Shivam Pandey*
Department of Chemistry, School of Applied and Life Sciences, Uttaranchal University, Dehradun-248007, India
*Corresponding author (e-mail: pandeyshivam547@gmail.com)

Recent emphasis has been directed on attaining the sustainable development goals by 2030. Given the significance of water and its numerous functions, the necessity for clean water is paramount. The inefficacy of many water treatment methods limits their extensive application. Consequently, it is imperative to devise an efficient and environmentally sustainable approach for transforming organic pollutants into non-toxic and innocuous substances. This research employed a green synthesis method from *Tradescantia spathacea* to successfully produce CuO nanoparticles. Fourier Transform Infrared (FT-IR) spectroscopy, X-Ray Diffraction (XRD), and Scanning Electron Microscopy (SEM) analysis were employed to characterize and elucidate the structural, morphological, and compositional properties of the synthesized nanoparticles. Furthermore, the synthesized particles were employed to decompose the harmful Bromocresol Green dye. At a concentration of 1 g/l of catalyst and basic medium, the degradation rate accelerated to 90-100% under UV light after approximately 80 minutes. When light was not present, the photocatalytic breakdown of bromocresol green using CuO nanoparticles was about half as effective as when light was present. The effectiveness of CuO nanoparticles that have been reused is maintained even after five cycles. Thus, the green synthesized catalysts are very practical, efficient, and stable.

Keywords: Copper Nanoparticles, photocatalytic activity, UV light, Bromocresol Green, *Tradescantia spathacea*

Received: March 2026; Accepted: March 2026

As the name suggests, "sustainable development" can be interpreted as "development which fulfil the needs of today's generation without jeopardizing next generations' potential to complete their own" [1]. Rapid industrial expansion driven by an ever-increasing population, has resulted in a rise in water consumption due to which water resources are severely contaminated and degraded [2-4]. Sustainable water management ensures safe drinking water amid climate, urban, and population challenges [5]. Heavy metals, oil residues, dyes, and polycyclic hydrocarbons all significantly degrade the quality of water.

Physical, chemical, and biological techniques are used in wastewater treatment to eliminate contaminants. Solids are separated by physical techniques like nanofiltration [6], microfiltration [7], reverse osmosis [8], forward osmosis [9], electrodialysis [10], centrifugal separation and screening along with filtration [11], gravity separation along with sedimentation [12, 13], adsorption [14, 15] etc. Chemical processes that neutralise or remove dissolved materials include coagulation [16], flotation [17], electrolysis [18], distillation [19], crystallization [20], evaporation [21] and advanced oxidation processes [22]. Microorganisms that decompose organic materials are used in biological procedures, frequently in biofilm or activated sludge processes [23, 24, 25, 26, 27]. By effectively addressing various contaminants, the combination of these methods guarantees cleaner water that is suitable for reuse or disposal. One of the major contaminants discharged from industries into the water bodies are dyes which majorly affects the human health and environment.

Colouring has been an important aspect of human vision for more than a century hence dyes are widely used in a variety of sectors, including printing, textiles, leather, plastics, coatings, food, and paper, hence industrial effluents containing dyes have a considerable impact on water contamination [28]. There are several dyes based on their nature such as natural dyes [29], synthetic dyes [30], reactive dyes [31, 32], direct dyes, vat dyes [33], acid dyes [34] and basic dyes [35]. Synthetic dyes are a major organic contaminant that frequently ends up in water streams. The presence of even minute amounts of such artificial dyes may cause enormous volumes of water to become coloured [30]. One such artificial dye that is a member of the triphenylmethane group is Bromocresol Green (BCG). It is a member of the sulfonephthalein dye class. In applications like titrations and microbe growth media, it serves as a pH indicator [36]. This ionic dye is usually found as a sodium salt (dark green solid),

†Paper presented at the International Conference on Chemistry and Sustainability, IC-CS 2025

which makes it very soluble in water and widespread contamination can be caused by even little amount of this dye in the plant's aqueous effluent. BCG can exist in two different forms based on the pH of the solution. In an aqueous solution, bromocresol green will ionise to produce the yellow monoanionic form, which will then deprotonate at a higher pH to produce the blue dianionic form. It has a blue hue above pH 5.4 and a yellow hue below pH 3.8 [37]. The structure of BCG is shown in Figure 1.

Dye chemicals are notoriously resistant to degradation and have been linked to a wide range of carcinogenic and mutagenic issues, providing a significant threat to both the environment and human health. As a result, dye-containing effluent must be treated before it is released into the environment [38, 39].

CuO nanomaterials, a p-type semiconductor, are regarded as exceptionally potential materials for utilisation in a range of industries, such as semiconductors, field-effect transistors and memory devices, solar energy, lithium-ion batteries, and photo catalysts for the breakdown of organic pollutants. CuO nanoparticle's small band gap enables them to efficiently absorb visible light making them useful as photo catalysts. Their large surface area, stability, and potent oxidation-reduction capabilities increase their effectiveness in breaking down organic contaminants and separating water for use in energy and environmental applications [45]. CuO NPs' durability and reusability add to their efficacy and make them a very economical and efficient option for wastewater treatment.

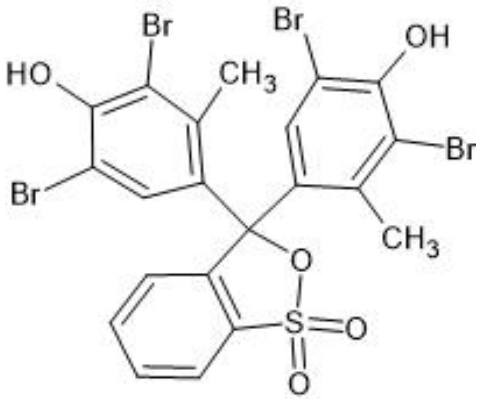

Figure 1. Molecular structure of Bromocresol Green.

Table 1. Comparison of metal oxide derived NPs for degradation of Bromocresol green.

S. No.	Type of Nanoparticles	Catalyst Dosage	BCG Concentration	% Degradation	Time (min)	References
1.	TiO_2 -PC500	1gm/mol	32 ppm	98%	180	[40]
2.	CaO-NPs	5gm	30 ppm	70%	60	[41]
3.	Co_3O_4-NPs	0.1gm	20 ppm	88%	300	[42]
4.	Ag-NPs	0.6gm	100 ppm	99.12%	30	[43]
5.	CaO-NPs	0.2gm	20 ppm	60%	180	[44]
6.	CuO-NPs (using *Tradescantia spathacea)*	1gm/L	100 ppm	100%	80	Present Work

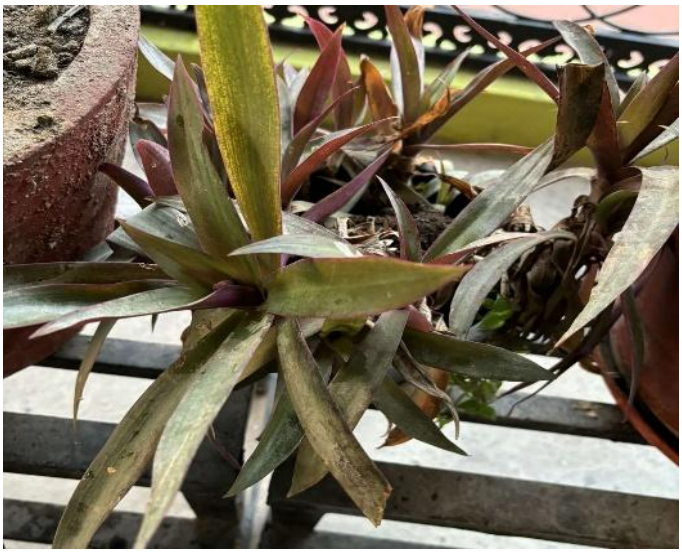

Figure 2. Plant sample of *Tradescantia Spathacea*.

Additionally, *Tradescantia spathacea*, a well-known species in traditional herbal medicine, has piqued researchers' interest due to its ability to cure a wide range of conditions. Studies have indicated that TS leaves contain antibacterial and antioxidant properties, supporting its traditional use for wounds, skin infections, fever, cancer, rhinitis, and respiratory diseases [46]. Around the world, several genera and species belonging to the *Commelinaceae* family have been identified and documented. These plants have been used historically for a variety of reasons, including food, decoration, religious ceremonies, medicine, and environmental aspects [47, 48]. However, two of the 75 species of *Tradescantia* are frequently used in bioactivity research. *Tradescantia* species are the most thoroughly researched and proved to have anti-cancerous activity [49,50], anti-viral activity [51], anti-inflammatory activity [52], antimycobacterial activity [53,54], and anti-oxidant properties [55,56].

In the current study, we have synthesized *Tradescantia spathacea* derived copper oxide nanoparticles and utilized them for degrading bromocresol green dye in presence of UV rays. The formed nanoparticles showed a 100% degradation efficiency in just 80 minutes. To the best of our knowledge no one has synthesized copper oxide nanoparticles and used them for degradation of bromocresol dye.

MATERIALS AND METHODOLOGY

Preparation of Leaf Extract

The plant *Tradescantia spathacea* was properly cleaned and dried in the sun. The leaf extract was then prepared by using the Soxhlet extraction method. The plant's leaves shown in Figure 2 were first sliced into small bits. The Soxhlet extractor was then set up with 15g of leaves inside a round bottom flask which was filled with 50ml of ethanol. The flask was then placed on a heating mantle. The process was repeated for 5-6 hours. Following the sample extraction, the sample was vapourised for 15-20 minutes on a hot plate, to make it more concentrated. It was then filtered and stored.

Green Synthesis of Copper Oxide Nanoparticles using Sol-Gel Method

In a 250ml beaker, 50ml of 1M aqueous copper oxide solution was used for biological production of copper oxide nanoparticles. 10ml of leaf extract was added to this and agitated at 80^0C for 2-3 hours before being left undisturbed. Nanoparticles were generated after few hours of incubation. The formed nanoparticles were then transferred to a petri-dish and heated for 10-15 minutes at 50 degrees Celsius. After that, the particles were placed in a hot air oven for about 2-3 hours for drying and later on they were cooled down, stored and utilized for further process. The process is explained briefly in Figure 3.

Photocatalytic Activity

The investigations of photocatalytic activity was carried out in a cylindrical glass beaker. A 100ml solution of bromocresol green dye (100ppm) with specified catalyst quantity was placed in a beaker and the pH of the reaction mixture was determined. The reaction mixture was then agitated for 30 minutes before being exposed to a UV lamp in UV inspection chamber as shown in Figure 4. A magnetic stirrer was utilized to keep the solution shaking throughout the experiment. After every fixed interval, 2-3ml of the solution was collected and centrifuged to extract the catalyst particles, and the solution was then analysed using UV-Visible spectroscopy.

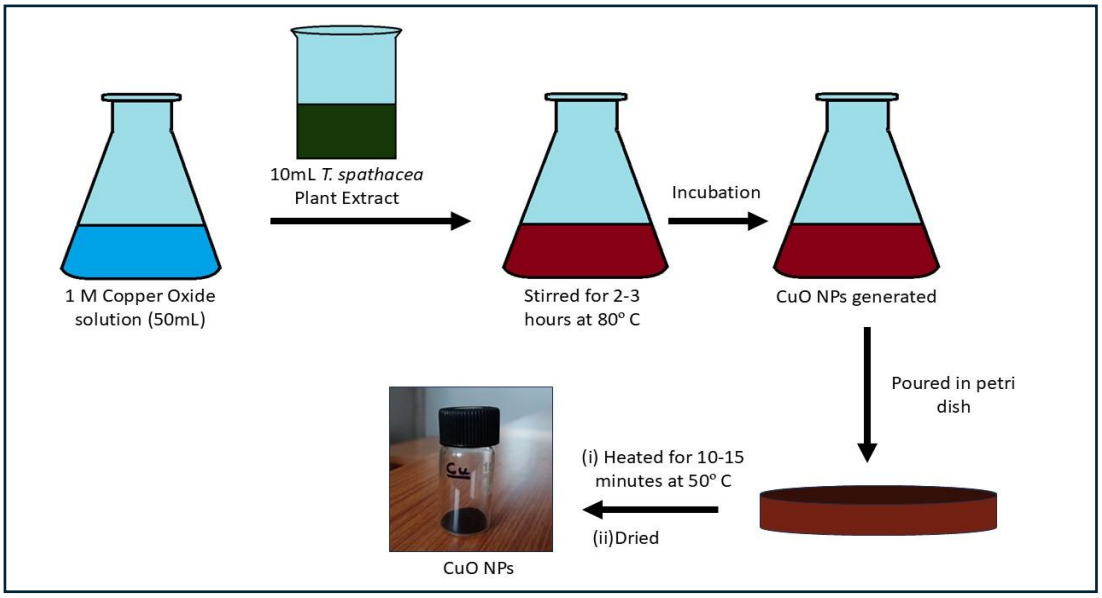

Figure 3. Prepared Copper Oxide Nanoparticles by Sol-Gel Method using Green synthesis.

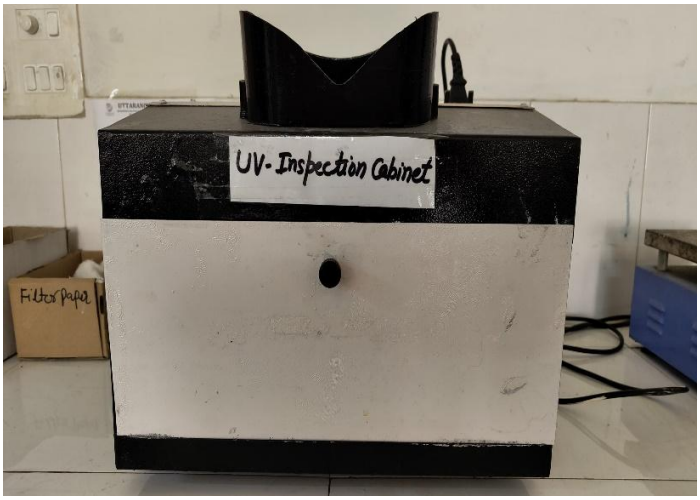

Figure 4. UV Inspection Cabinet.

The extent of degradation by synthesised catalysts was determined using the equation below.

$$\% \ Degradation = C_0\text{-}C_t / C_0 * 100 \quad (1)$$

where C_0 and C_t are the starting and final concentrations obtained under the same reaction conditions.

Photocatalytic Degradation Mechanism

The primary process of photocatalytic degradation by copper oxide nanoparticles (CuO NPs) is the absorption of light energy, usually in the visible or ultraviolet spectrum, because of CuO's small bandgap. CuO NPs absorb photons when exposed to radiation, which causes electrons in the valence band to be excited and move into the conduction band. With electrons (e^-) in the conduction band and holes (h^+) in the valence band, this process creates electron-hole pairs. For the photocatalytic processes to begin, these electron-hole pairs are essential.

$$CuO + hv \rightarrow CuO(e\text{-}) + CuO(h+) \quad (2)$$

The conduction band's excited electrons have the ability to interact with nearby oxygen molecules (O_2) and reduce them to create superoxide radicals

($\bullet O_2^-$). In the meanwhile, hydroxyl radicals ($\bullet OH$) can be created when the valence band holes interact with water molecules on the CuO NPs' surface.

$$CuO(e\text{-}) + O_2 \rightarrow \bullet O_2^- \quad (3)$$

$$CuO(h+) + H_2O \rightarrow \bullet OH \quad (4)$$

Superoxide and hydroxyl radicals are the primary oxidising agents in the breakdown process and are both extremely reactive. By attacking the pollutant molecules, these reactive oxygen species (ROS) disassemble complex organic structures into smaller, less dangerous intermediates.

$$\text{Dye} + \bullet O_2^- \rightarrow \text{Degraded Products } (CO_2 + H_2O) \leftarrow \text{Dyes} + \bullet OH \quad (5)$$

These intermediates are eventually mineralised into Carbon dioxide (CO_2), Water (H_2O), and other innocuous by-products by a series of oxidation processes as shown in Figure 5.

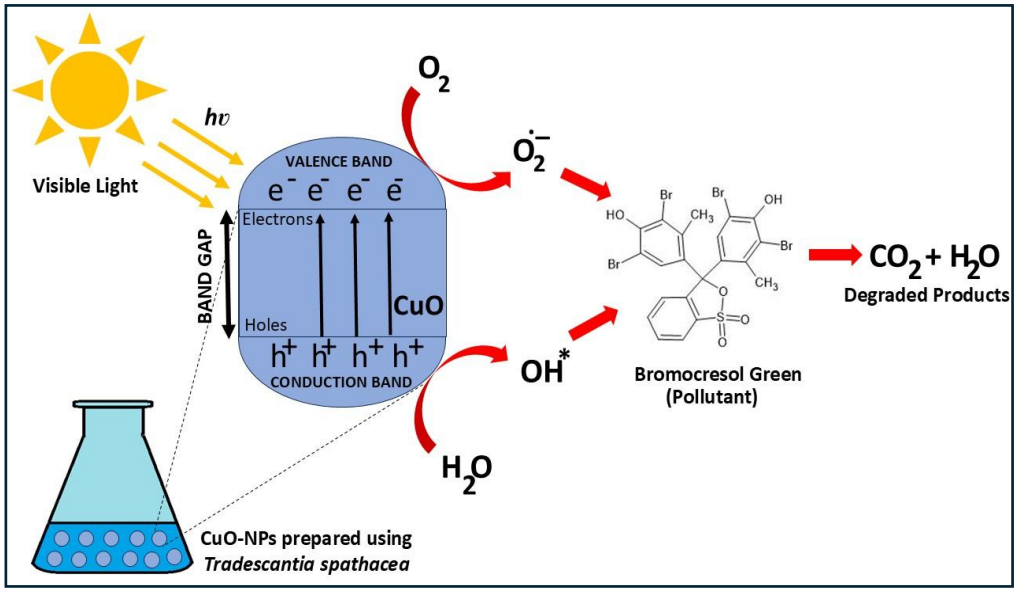

Figure 5. Photocatalytic degradation mechanism.

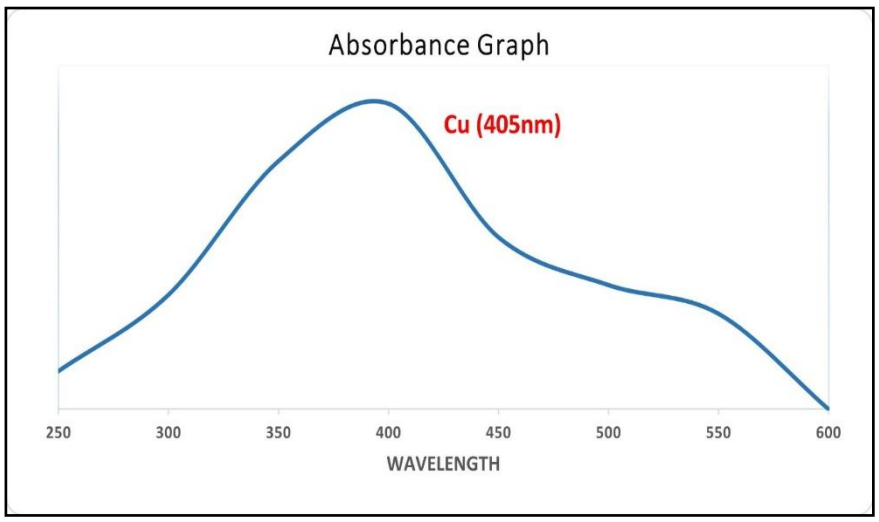

Figure 6. UV-Visible Spectrum of prepared CuO Nanoparticles.

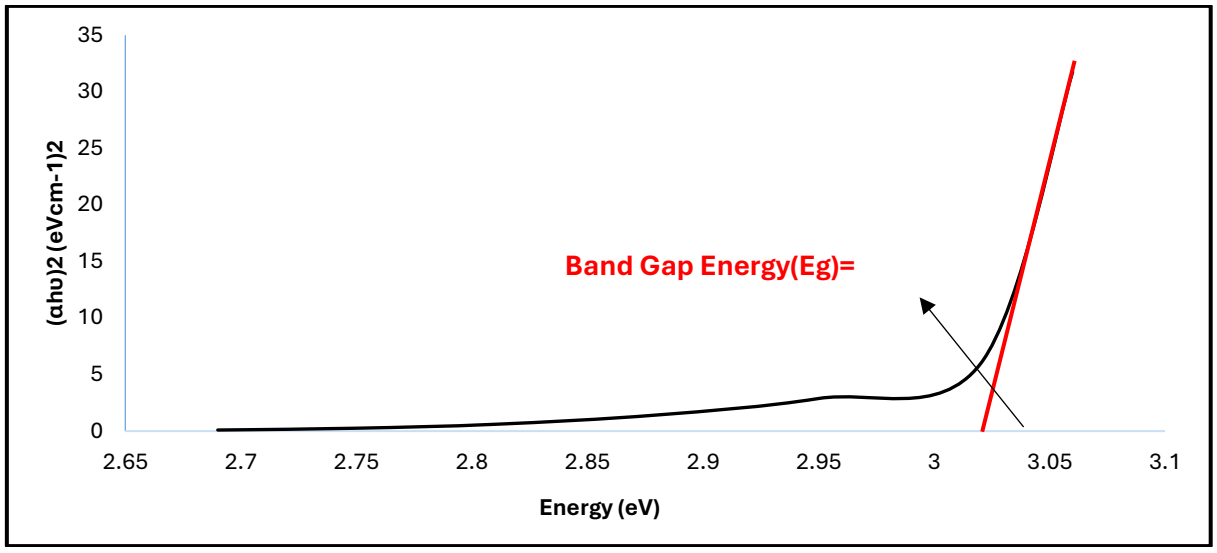

Figure.7. Tauc Plot.

RESULT AND DISCUSSIONS

Characterisation

The formation of nanoparticles was confirmed by using UV-Visible spectroscopy. In the UV–Vis spectra of the CuO NPs, the production of CuO NPs is indicated by the most prominent absorption peaks at 380–450 nm. The spectra's highest peak is attributed to the shift in surface plasmon resonance (SPR) caused by metal oxide absorption. The highest peak, which confirmed the production of CuO NPs was seen at 405 nm as seen in Figure.6. The Tauc plot has been employed for calculating the nanoparticles bandgap energy.

The Tauc equation is represented as:

$$(\alpha h\upsilon)^{\gamma} = A(h\upsilon - E_g) \quad (6)$$

where hυ is the energy of the incident photon, α is absorption coefficient of the material, E_g is the band gap energy, A is the proportionality constant and γ denoted the nature of the electronic transition, γ=2 (direct allowed transition). The band gap energy of the direct transition of CuO nanoparticles was determined using a tauc plot to be Eg = 3.025eV as shown in Figure.7, demonstrating the high photocatalytic activity of the material that was synthesised at the nanoscale.

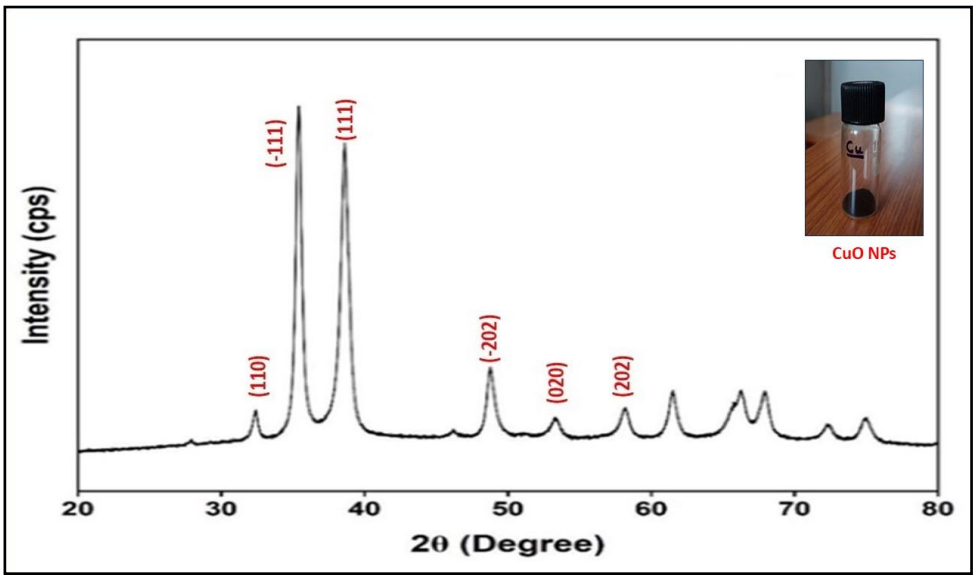

Figure 8. XRD Pattern of Copper Oxide.

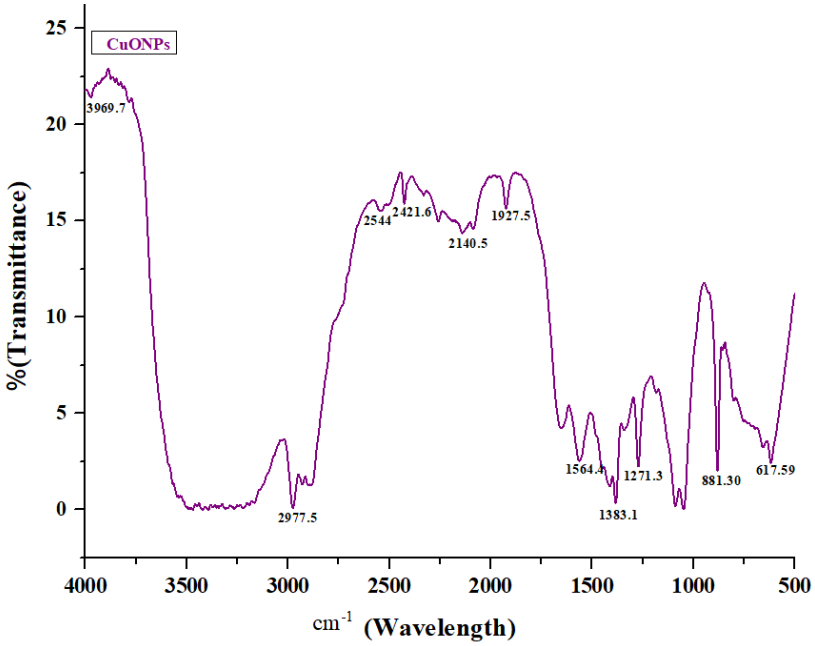

Figure 9. FTIR Spectrum of Copper Oxide.

XRD is an effective and frequently used material characterisation tool [57]. XRD pattern of CuO Nanoparticles is shown in Figure.8. It was determined that the Copper Oxide i.e. CuO, nanomaterial has a monoclinic structure by obtaining diffraction peaks at 2Θ values of 32.3^0, 35.2°, 38.4°, 48.6°, 53.3°, 58.2° parallel to (110), (111), (111), (202), (020), and (202) planes. Sharp diffraction peaks between (2Θ = 35.5-38.6) are seen, confirming that CuO NPs were successfully synthesised. The current findings align with earlier publications on CuO synthesis [58, 59].

FTIR microscopy is well recognized as a useful tool for micro-destructive testing of small materials. Recent developments in mapping and imaging technologies have enabled the capture of several FTIR spectra on a single surface, providing a distribution map of known compounds [60].

Fourier Transform Infrared (FTIR) spectroscopy was conducted to analyze the functional groups of the synthesized copper oxide nanoparticles (CuO NPs) and to verify their formation. FTIR spectrum was taken in the 4000 -500 cm^{-1} range, and the observed bands are in line with the previously reported articles on CuO nanoparticles. The wide absorption band at 3969 cm^{-1} can be attributed to OH stretching vibrations that could be a result of surface-adsorbed water and hydroxyl groups attached to the CuO surface. This type of hydroxyl group is usually reported in CuO nanoparticles and helps to make them surface reactive and stable [61,62]. This peak at the value of approximately 2977cm^{-1} is assigned to the aliphatic CH stretching vibrations, and in this case, it is due to the remaining organic species on the surface of the CuO nanoparticles. The same has been observed in the case of chemically and biologically prepared CuO nanoparticles [63]. The low intensity bands at 2544 cm^{-1} and 2421 cm^{-1} can be attributed to the O-H stretch of carboxylic or a CO_2 adsorption in the weak band, which is very common in CuO nanostructure that has been exposed to the ambient conditions [64]. The absorption band at 2140 cm^{-1} can be attributed to functional groups of unsaturated functional groups stretching, and the band at 1927 cm^{-1} is associated with combination or overtone bands of organic residues bound on the surface, as cited in CuO nanoparticle FTIR spectra [65].

It is observed that a significant peak at the position of 1564 cm^{-1} corresponds to N-H bending or C=C vibrations, which is evidence of the presence of functional groups of surface elements in contact with the nanoparticles of CuO. The highest point at 1383 cm^{-1} can be attributed to symmetric stretching of carboxylate groups (-COO -), which indicates that the copper ions are coordinated with surface ligands [66]. Absorption band at 1271 cm^{-1} is attributed to C -O stretching vibrations, and the intense band at 881 cm^{-1} is attributed to C -H bending vibrations. Notably, the high absorption band at 617 cm^{-1} resembles the Cu -O stretching vibrations, which are conclusive to form copper oxide nanoparticles. This CuO vibrational band is one of the main fingerprints of monoclinic CuO that has been extensively reported on in the CuO nanoparticle literature [67-69]. In general, the FTIR data prove the effective synthesis of CuO nanoparticles.

SEM examination is used to classify the size, morphologies and form of nanoparticles that are created. SEM is used to obtain high resolution pictures of a sample's surface. SEM analysis showed that the formed NPs particles have spherical morphology and are agglomerated as seen in Figure 10.

Photocatalytic Degradation

Synthesised CuO Nanoparticles were used for the degradation of Bromocresol Green dye in presence of UV light. Different parameters such as concentration of catalyst, concentration of pollutant and pH were varied and the experimental results were observed.

Effect of Time

Figure 11. illustrates the photocatalytic degradation of Bromocresol Green dye under different time period. The experiments was performed to verify the effectiveness of NPs on dye degradation. 0.1g/l of catatlyst dose was used for 100 ppm solution of the dye. The % degradation of the taken dye was only 10% under light after 10 minutes. But within a time of about 80 minutes, the degradation percentage increased up to 100% under UV light. Our result is similar to Rocha et al., who concluded in their work that with increase in time, % degradation also increases [70].

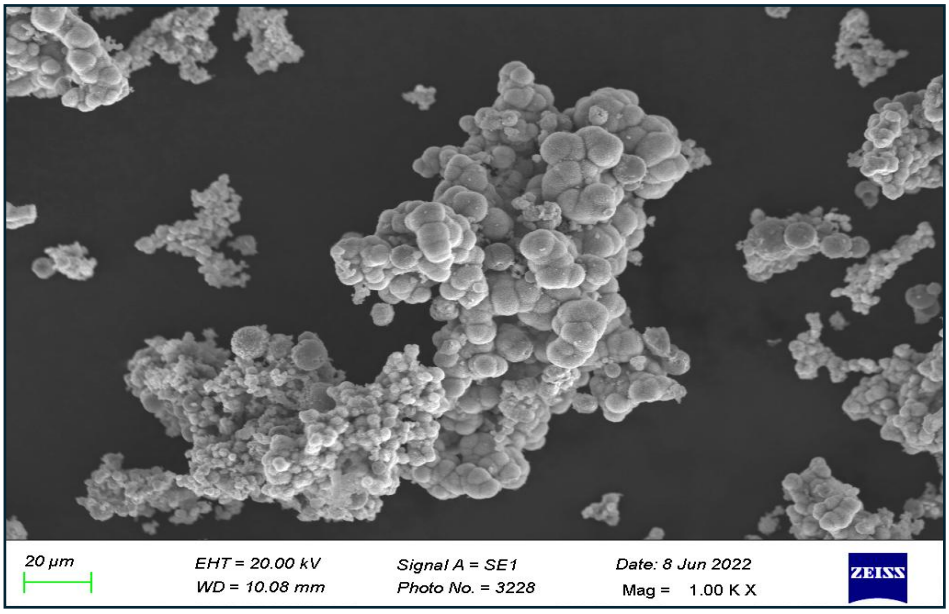

Figure 10. SEM image of CuO Nanoparticles.

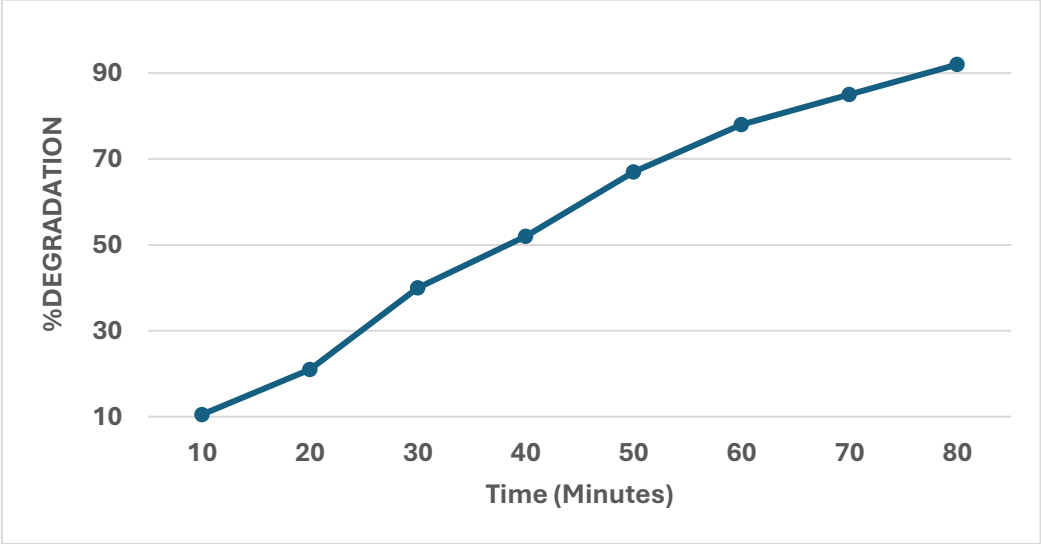

Figure 11. Effect of time on the degradation of Bromocresol Green.

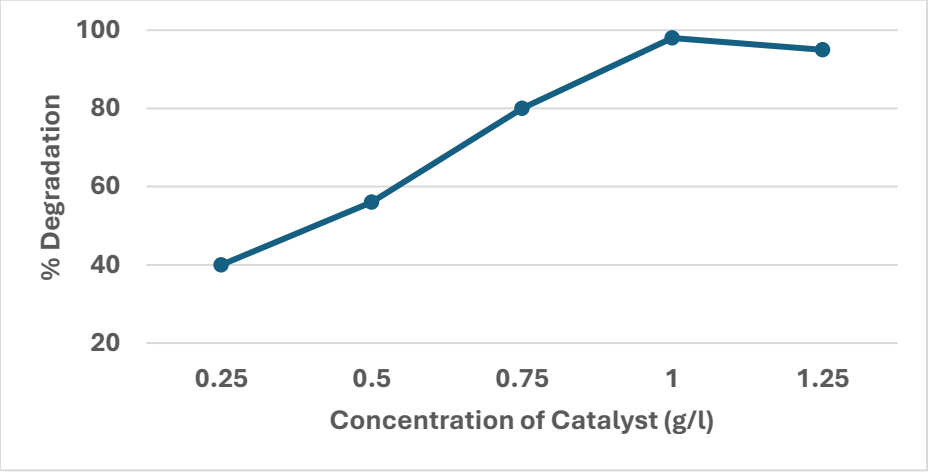

Figure 12. Effect of varying concentration of catalyst on the degradation of Bromocresol Green.

Concentration of Catalyst

Figure 12 reported the photocatalytic degradation of Bromocresol Green under different concentration of catalyst. According to the analysis, with increase in concentration of the catalyst the percentage of degradation also increases. The observation of graph states that at 0.25 g/l concentration, the percent of degradation is only 35-40%. But as the concentration of the catalyst is increased the degradation percent also starts increasing. The percent degradation of the dye touches almost 100% at concentration of 1g/l. After further increase in the concentration the degradation starts decreasing slowly and reduces to a value of 95%. Our observation is similar to El-Kammah et al., who observed that there is maximum degradation at 1g/l solution [71]. This behavior results from an increase in the number of active sites and photons continually absorbed on the catalyst particle's surface, hence enhancing the degradation percentage. However, when the catalyst concentration surpasses the ideal level, particle agglomeration occurs, leading to a reduction in surface area and thus diminishing the catalyst's degrading efficiency.

Effect of pH

As per observation via Figure.13, in acidic medium the degradation is lesser upto 50% and it increase as the pH increase. The degradation was found to be maximum 90-100% in the basic medium. At neutral pH, the degradation is about 67-70%. Kim et al., also observed the similar trend in their work that with increase in pH, % degradation will also increase [72].

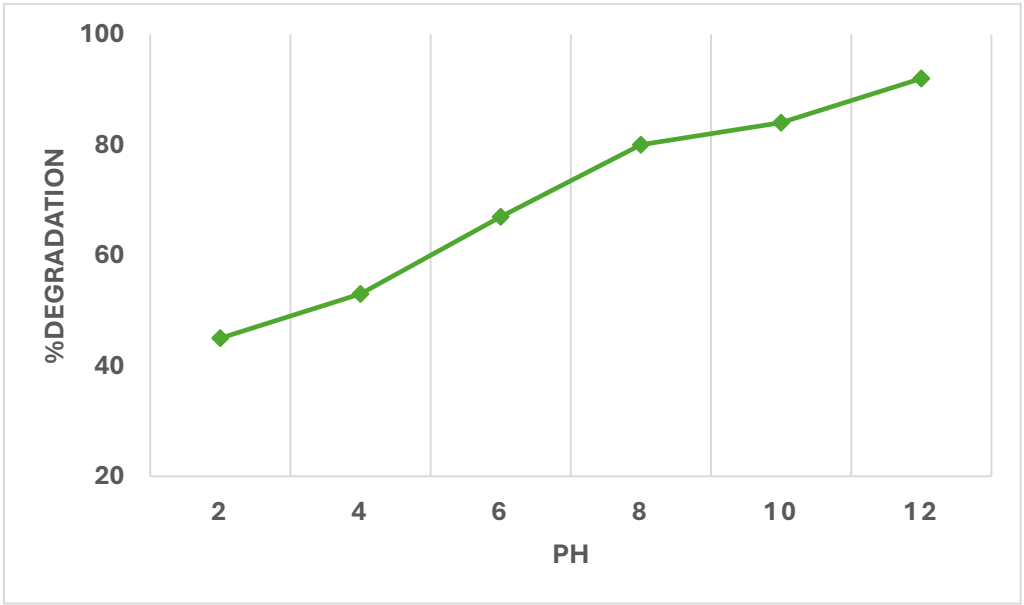

Figure 13. Effect of varying pH on the degradation of Bromocresol Green.

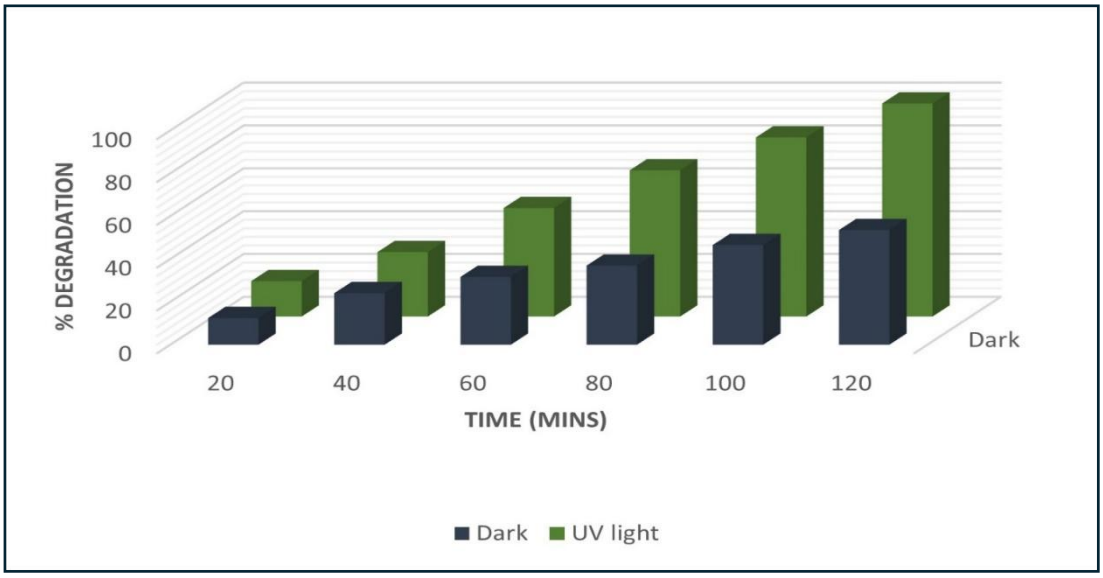

Figure 14. Effect of light condition on degradation of dye.

When assessing materials or techniques intended for the removal of dye from water or effluent, the degradation of dye in the presence and absence of UV radiation is usually used to gauge the efficacy of photocatalytic processes. In overcast or dark situations, UV light could not be available for wastewater cleanup. Knowing how well the degrading process works without UV light makes it easier to assess its viability and scalability in a range of environmental conditions. The results of the experiment demonstrated that when photocatalytic degradation conducted in the dark, the CuO NPs was about half as effective as when photocatalytic degradation when done in presence of light as illustrated in Figure 14.

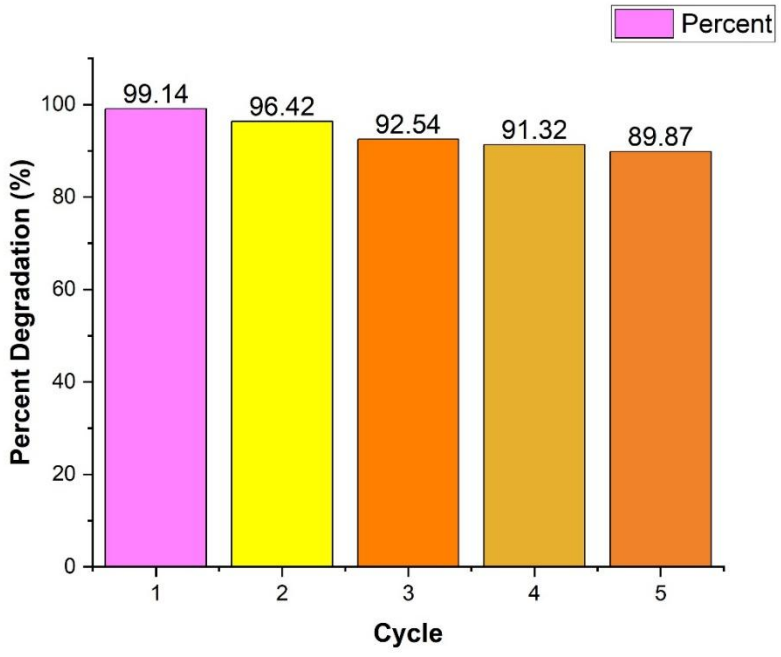

Figure 15. Reusability of formed catalyst.

Reusability

Two critical and significant aspects of study are the recovery and reusability of the CuO photo catalyst following the photocatalytic experiment. Reusing CuO nanoparticles is made feasible by the CuO photo catalyst's easy separation from the reaction mixture. At the conclusion of each step, the CuO catalyst was extracted from the reaction mixture, cleaned with ethanol and water, dried in a vacuum oven, and then used in the subsequent degrading cycles at room temperature. The cycle was repeated five times ≥99% dyes were degraded in 1st series which gradually decreased per cycle as 96.42%, 92.54%, 91.32%, 89.87% for 2nd, 3rd, 4th and 5th cycles, respectively as illustrated in Figure 15. Consequently, the sol gel synthesised CuO nanoparticles high catalytic efficiency, stability, and ease of recycling allow it to be a viable photocatalyst for ecological restoration.

CONCLUSION

We successfully synthesized copper oxide nanoparticles utilizing leaf extracts from *Tradescantia spathacea*. Following the synthesis of CuO nanoparticles, we degrade Bromocresol Green dye by using them, facilitating various observations by experimental techniques. The XRD pattern indicated that the Copper Oxide nanomaterial possessed a monoclinic structure, exhibiting the strongest diffraction peaks at 2Ɵ values ranging from 35.5° to 38.6°. SEM analysis indicated that the CuO nanoparticles exhibited a spherical morphology. Synthesized CuO nanoparticles were also utilized to decompose Bromocresol Green under various parameters. After around 80 minutes, the deterioration rate escalated to 90-100% under UV light with the peak degradation seen at a concentration of 1 g/l solution and basic medium. Degradation will be most pronounced in a basic solution with respect to pH. The photocatalytic degradation of bromocresol green in the absence of light demonstrated that CuO nanoparticles were approximately half as effective compared to degradation conducted in the presence of light. The reusability of CuO nanoparticles is highly effective even after five cycles. The synthesized catalysts exhibit exceptional stability, efficiency, and economic viability.

REFERENCES

1. Bhaduri, A., Bogardi, J., Siddiqi, A., Voigt, H., Vörösmarty, C., Pahl-Wostl, C., Bunn, S. E., Shrivastava, P., Lawford, R., Foster, S., Kremer, H., Renaud, F. G., Bruns, A. and Osuna, V. R. (2016) Achieving sustainable development goals from a water perspective. *Frontiers in Environmental Science*, **4**, 64.

2. Rahman, T. U., Roy, H., Islam, M. R., Tahmid, M., Fariha, A., Mazumder, A., Nahar, N., Hossain, M. T., Rahman, M. M. and Islam, M. S. (2023) The advancement in membrane bioreactor (MBR) technology toward sustainable industrial wastewater management. *Membranes*, **13(2)**, 181.

3. Zhang, C. Y. and Oki, T. (2023) Water pricing reform for sustainable water resources management in China's agricultural sector. *Agricultural Water Management*, **275**, 108045.

4. Sahoo, S. and Goswami, S. (2024) Theoretical framework for assessing the economic and environmental impact of water pollution: A detailed study on sustainable development of India. *Journal of Future Sustainability*, **4(1)**, 23–34.

5. Van de Walle, A., Kim, M., Alam, M. K., Wang, X., Wu, D., Dash, S. R., Van Dessel, J., Dhakal, D. and Kim, J. (2023) Greywater reuse as a key enabler for improving urban wastewater management. *Environmental Science and Ecotechnology*, 100277.

6. Bóna, Á., Galambos, I. and Nemestóthy, N. (2023) Progress towards stable and high-performance polyelectrolyte multilayer nanofiltration membranes for future wastewater treatment applications. *Membranes*, **13(4)**, 368.

7. Laurell, P., Poutanen, H., Hesampour, M., Tuutijärvi, T. and Vahala, R. (2023) Feasibility and environmental impact of NOM reduction by microfiltration at a Finnish surface water treatment plant. *Water*, **15(10)**, 1822.

8. Malaeb, L. and Ayoub, G. M. (2011) Reverse osmosis technology for water treatment: State of the art review. *Desalination*, **267(1)**, 1–8.

9. Lutchmiah, K., Verliefde, A. R. D., Roest, K., Rietveld, L. C. and Cornelissen, E. R. (2014) Forward osmosis for application in wastewater treatment: A review. *Water Research*, **58**, 179–197.

10. Gurreri, L., Tamburini, A., Cipollina, A. and Micale, G. (2020) Electrodialysis applications in wastewater treatment for environmental protection and resources recovery: A systematic review on progress and perspectives. *Membranes*, **10(7)**, 146.

11. Pandey, S., Lingwal, M. and Painuli, R. (2025) Historical development of photocatalyst and its application in water purification. *In Metal Oxide Based Nanophotocatalyst for Wastewater Purification*, 355–376.

12. Jaiswal, S., Sharma, R., Jangid, N. K. and Dwivedi, J. (2024) Photonanocatalyst for water purification, in Nanotechnology to Monitor, Remedy, and Prevent Pollution. *Elsevier*, 295–321.

13. Frising, T., Noïk, C. and Dalmazzone, C. (2006) The liquid/liquid sedimentation process: From droplet coalescence to technologically enhanced water/oil emulsion gravity separators: A review. *Journal of Dispersion Science and Technology*, **27(7)**, 1035–1057.

14. Burakov, A. E., Galunin, E. V., Burakova, I. V., Kucherova, A. E., Agarwal, S., Tkachev, A. G. and Gupta, V. K. (2018) Adsorption of heavy metals on conventional and nanostructured materials for wastewater treatment purposes: A review. *Ecotoxicology and Environmental Safety*, **148**, 702–712.

15. Nayak, A., Bhushan, B. and Kotnala, S. (2024) Fundamentals and mechanism of adsorption, in Sustainable Remediation Technologies for Emerging Pollutants in Aqueous Environment. *Elsevier*, 29–62.

16. Sheng, D. P. W., Bilad, M. R. and Shamsuddin, N. (2023) Assessment and optimization of coagulation process in water treatment plant: A review. *ASEAN Journal of Science and Engineering*, **3(1)**, 79–100.

17. Alhuseen, A., Noori, H. and Abdulrazzaq, N. N. (2023) Flotation of cadmium ions from wastewater using air micro-bubbles. *Journal of Ecological Engineering*, **24(8)**.

18. Chopra, A. K., Sharma, A. K. and Kumar, V. (2011) Overview of electrolytic treatment: An alternative technology for purification of waste-water. *Archives of Applied Science Research*, **3(5)**, 191–206.

19. Wilk, M., Czerwińska, K., Śliz, M. and Imbierowicz, M. (2023) Hydrothermal carbonization of sewage sludge: Hydrochar properties and processing water treatment by distillation and wet oxidation. *Energy Reports*, **9**, 39–58.

20. Jebur, M., Bachynska, Y., Hao, X. and Wickramasinghe, S. R. (2023) Integrated electro-coagulation, ultrafiltration, membrane distillation, and crystallization for treating produced water. *Membranes*, **13(6)**, 597.

21. Zhao, F., Guo, Y., Zhou, X., Shi, W. and Yu, G. (2020) Materials for solar-powered water evaporation. *Nature Reviews Materials*, **5(5)**, 388–401.

22. Gomes, J., Costa, R., Quinta-Ferreira, R. M. and Martins, R. C. (2017) Application of ozonation for pharmaceuticals and personal care products removal from water. *Science of the Total Environment*, **586**, 265–283.

23. Lawal, I. M., Soja, U. B., Hussaini, A., Saleh, D., Aliyu, M., Noor, A. and Jagaba, A. H. (2023) Sequential batch reactors for aerobic and anaerobic dye removal: A mini-review. *Case Studies in Chemical and Environmental Engineering*, 100547.

24. Yang, Y., Guo, W., Ngo, H. H., Zhang, X., Liang, S., Deng, L. and Zhang, H. (2024) Bioflocculants in anaerobic membrane bioreactors: A review on membrane fouling mitigation strategies. *Chemical Engineering Journal*, 150260.

25. Grady Jr., C. L., Daigger, G. T., Love, N. G. and Filipe, C. D. (2011) Biological Wastewater Treatment. *CRC Press*.

26. van Loosdrecht, M. C., Nielsen, P. H., Lopez-Vazquez, C. M. and Brdjanovic, D. (2016) Experimental Methods in Wastewater Treatment. *IWA Publishing (Eds.)*.

27. Chan, Y. J., Chong, M. F., Law, C. L. and Hassell, D. G. (2009) A review on anaerobic–aerobic treatment of industrial and municipal wastewater. *Chemical Engineering Journal*, **155(1–2)**, 1–18.

28. de Campos Ventura-Camargo, B. and Marin-Morales, M. A. (2013) Azo dyes: Characterization and toxicity-a review. *Textiles and Light Industrial Science and Technology*, **2(2)**, 85–103.

29. Jabar, J. M. (2024) Classification of natural dyes for sustainable exploitation, in Natural Dyes and Sustainability. *Springer Nature Switzerland, Cham.*, 153–191.

30. Millbern, Z., Trettin, A., Wu, R., Demmler, M. and Vinueza, N. R. (2024) Synthetic dyes: A mass spectrometry approach and applications. *Mass Spectrometry Reviews*, **43(2)**, 327–344.

31. Zhao, W., Rong, Y., Xu, R. & Wu, Y. (2024) Study on transparent basswood dyed with reactive dyes and its properties. *ACS Omega*, **9(5)**, 5378-5385.

32. Li, D., Gao, Z., Zhang, B., Ma, W., Tang, B. and Zhang, S. (2024) Excellent fixation of low-water-soluble reactive dyes containing vinylsulfone group for nylon dyeing. *Dyes and Pigments*, 222, 111887.

33. Shi, B., Li, G., Wang, D., Feng, C. and Tang, H. (2007) Removal of direct dyes by coagulation: The performance of preformed polymeric aluminum species. *Journal of Hazardous Materials*, 143(1–2), 567–574.

34. Nayfert, S. A., Sakthidharan, C. P., Dorovatovsky, P. V., Efremov, A. N., Osipov, A. A., Rajakumar, K. and Zherebtsov, D. A. (2024) Structure of four vat dyes and of violanthrene. *Dyes and Pigments*, **222**, 111839.

35. Hunger, K. (2007) Industrial Dyes: Chemistry, Properties, Applications. *John Wiley & Sons (Ed.)*.

36. Onu, C. E., Ohale, P. E., Ekwueme, B. N., Obiora-Okafo, I. A., Okey-Onyesolu, C. F., Onu, C. P. and Onu, O. O. (2022) Modeling, optimization, and adsorptive studies of bromocresol green dye removal using acid functionalized corn cob. *Cleaner Chemical Engineering*, **4**, 100067.

37. Elijah, O. C., Collins, O. N., Obumneme, O. C. and Jessica, N. B. (2020) Application of modified agricultural waste in the adsorption of bromocresol green dye. *Asian Journal of Chemical Sciences*, **7(1)**, 15–24.

38. Tsoutsa, E. K., Tolkou, A. K., Kyzas, G. Z. and Katsoyiannis, I. A. (2024) An update on agricultural wastes used as natural adsorbents or coagulants in single or combined systems for the removal of dyes from wastewater. *Water, Air, and Soil Pollution*, **235(3)**, 1–21.

39. Mishra, M., Urooj, T., Singh, A. and Pandey, S. (2024) A new approach for synthesis of bismuth oxide derived photocatalyst for degradation of para nitrophenol. *Desalination and Water Treatment*, **319**, 100558.

40. Fassi, S., Djebbar, K. and Sehili, T. (2014) Photocatalytic degradation of bromocresol green by TiO2/UV in aqueous medium. *Journal of Materials and Environmental Science*, **5**, 1093–1098.

41. Ogoko, E. C., Kelle, H. I., Akintola, O. and Eddy, N. O. (2024) Experimental and theoretical investigation of Crassostrea gigas shells based CaO nanoparticles as a photocatalyst for the degradation of bromocresol green dye (BCGD) in an aqueous solution. *Biomass Conversion and Biorefinery*, **14(13)**, 14859–14875.

42. Dinka, W. F. and Regasa, M. B. (2024) Cobalt oxide-zinc oxide nanocatalysts loaded on activated carbon for the photocatalytic degradation of methylene blue dye in water.

43. Aljubiri, S. M., El-Shwiniy, W. H., Younes, A. A., Alosaimi, E. H. and El-Wahaab, B. A. (2023) Use of Euphorbia balsamifera extract in precursor fabrication of silver nanoparticles for efficient removal of bromocresol green and bromophenol blue toxic dyes. *Molecules*, **28(9)**, 3934.

44. Osuntokun, J., Onwudiwe, D. C. and Ebenso, E. E. (2018) Aqueous extract of broccoli mediated synthesis of CaO nanoparticles and its application in the photocatalytic degradation of bromocresol green. *IET Nanobiotechnology*, **12(7)**, 888–894.

45. Singh, J., Kumar, V., Kim, K. H. and Rawat, M. (2019) Biogenic synthesis of copper oxide nanoparticles using plant extract and its prodigious potential for photocatalytic degradation of dyes. *Environmental Research*, **177**, 108569.

46. Lim, B. C. W., Keng, X. Y., Loh, K. E. and Tan, S. P. (2023) Determination of antioxidant and antibacterial properties of Tradescantia spathacea root extracts. *Vegeto*s, **36(4)**, 1475–1482.

47. Tan, J. B. L. and Kwan, Y. M. (2020) The biological activities of the spiderworts (Tradescantia). *Food Chemistry*, **317**, 126411.

48. Tan, S. P., Keng, X. Y., Chi-Wah Lim, B. and Tan, H. Y. (2024) Traditional uses, phytochemistry and pharmacological activities of Tradescantia spathacea. *Records of Natural Products*, 18(2).

49. Prakash, R. and Rajesh, R. (2014) Aberrant expression of WNT/Beta-catenin signaling pathway and in-vitro cytotoxic activity of Tradescantia spathacea medicinal plant used to treat human breast adenocarcinoma (MCF-7 cell lines). *International Journal of Pharmaceutical Sciences and Research*, **5**, 5230–5234.

50. Seca, A. M. and Pinto, D. C. (2018) Plant secondary metabolites as anticancer agents: Successes in clinical trials and therapeutic application. *International Journal of Molecular Sciences*, **19(1)**, 263.

51. Imtiyaz, A. and Singh, A. (2025) Pharmacological and photocatalytic study of green synthesized cobalt oxide (Co3O4) nanoparticles using Iris kashmiriana plant extract. *Next Research*, **2(2)**, 100329.

52. Pulipaka, S., Suttee, A., Kumar, M. R. and Sriram, P. (2020) A review on phytopharmacological activities of Alpinia mutica and Tradescantia spathacea. *Plant Archives*, **20(2)**, 9011–9018.

53. García-Varela, R., García-García, R. M., Barba-Dávila, B. A., Fajardo-Ramírez, O. R., Serna-Saldívar, S. O. and Cardineau, G. A. (2015) Antimicrobial activity of Rhoeo discolor phenolic rich extracts determined by flow cytometry. *Molecules*, **20(10)**, 18685–18703.

54. Radji, M., Kurniati, M. and Kiranasari, A. (2015) Comparative antimycobacterial activity of some Indonesian medicinal plants against multi-drug

resistant Mycobacterium tuberculosis. *Journal of Applied Pharmaceutical Science*, **5(1)**, 019–022.

55. Misin, V. M. and Sazhina, N. N. (2010) Content and activity of low-molecular antioxidants in juices of medicinal plants. *Russian Journal of Physical Chemistry* B, **4**, 797–800.

56. Reyes-Munguía, A., Azúara-Nieto, E., Beristain, C. I., Cruz-Sosa, F. and Vernon-Carter, E. J. (2009) Purple maguey (Rhoeo discolor) anti-oxidant properties. *CyTA–Journal of Food*, **7(3)**, 209–216.

57. Ali, A., Chiang, Y. W. and Santos, R. M. (2022) X-ray diffraction techniques for mineral characterization: A review for engineers of the fundamentals, applications, and research directions. *Minerals*, **12(2)**, 205.

58. Nezamzadeh-Ejhieh, A. and Amiri, M. (2013) CuO supported clinoptilolite towards solar photocatalytic degradation of p-aminophenol. *Powder Technology*, **235**, 279–288.

59. Akintelu, S. A., Folorunso, A. S., Folorunso, F. A. and Oyebamiji, A. K. (2020) Green synthesis of copper oxide nanoparticles for biomedical application and environmental remediation. *Heliyon*, **6(7)**.

60. Prati, S., Joseph, E., Sciutto, G. and Mazzeo, R. (2010) New advances in the application of FTIR microscopy and spectroscopy for the characterization of artistic materials. *Accounts of Chemical Research*, **43(6)**, 792–801.

61. Barreca, D., Gasparotto, A. and Tondello, E. (2007) Structural and optical properties of CuO nanostructures, *Nanotechnology*, **18,** 125701.

62. Rakhshani, A. E. and Makdisi, Y. (1986) Electronic and optical properties of CuO films. *Journal of Applied Physics*, **60**, 2474–2477.

63. Zhang, Q., Zhang, K., Xu, D., Yang, G., Huang, H., Nie, F., Liu, C. and Yang, S. (2014) *Prog. Mater. Sci.*, **60**, 208–337.

64. Wang, Z. L. (2000) Characterization of Nanophase Materials. *Wiley-VCH, Germany*.

65. Sahar, M. R. and El-Sayed, M. A. (2012) FTIR analysis of CuO nanoparticles. *Applied Surface Science*, **258**, 6399–6404.

66. Abdollahzadeh-Ghom, S. and Zamani, C. (2015) Surface chemistry of CuO nanoparticles. *Ceramics International*, **4**1, 154–160.

67. Shanmugam, N. and Cholan, S. (2014) Green synthesis of CuO nanoparticles and their characterization. *Spectrochimica Acta Part A*, **133**, 471–476.

68. Azam, A., Ahmed, A. S., Oves, M., Khan, M. S., Habib, S. S. and Memic, A. (2012) Antimicrobial activity of CuO nanoparticles. *International Journal of Nanomedicine*, **7**, 3527–3535.

69. Phiwdang, K., Suphankij, S., Mekprasart, W. and Pecharapa, W. (2013) Synthesis of CuO nanoparticles by the precipitation method. *Energy Procedia*, **34**, 740–745.

70. Kandari, D. and Pandey, S. (2024) Comparative study of photocatalytic activity of Tinospora cordifolia derived nanoparticles for degradation of indigo carmine. *Desalination and Water Treatment*, **320**, 100870.

71. El-Kammah, M., Elkhatib, E., Gouveia, S., Cameselle, C. and Aboukila, E. (2022) Cost-effective ecofriendly nanoparticles for rapid and efficient indigo carmine dye removal from wastewater: Adsorption equilibrium, kinetics and mechanism. *Environmental Technology and Innovation*, **28**, 102595.

72. Kim, C. M., Chowdhury, M. F., Im, H., Cho, K. and Jang, A. Adsorptive photocatalytic reaction on NiAlFe LDH/MoS2 photocatalyst using Z-scheme heterojunction for enhanced degradation of organic dye under high alkaline conditions. *SSRN*, 4713450.